# Prickle and Strabismus form a functional complex to generate a correct axis during planar cell polarity signaling

**Andreas Jenny, Rachel S.Darken[1], Paul A.Wilson[2] and Marek Mlodzik[3]**

Mount Sinai School of Medicine, Brookdale Department of Molecular, Cellular and Developmental Biology, 1 Gustave L.Levy Place, New York, NY 10029, USA

[1]Present address: Weill Medical College, Department of Cell and Molecular Biology, 1300 York Avenue, New York, NY 10021, USA
[2]Present address: Earth Institute, CSPO, 1 Thomas Circle, NW Suite 1075, Washington, DC 20005, USA

[3]Corresponding author
e-mail: marek.mlodzik@mssm.edu

**Frizzled (Fz) signaling regulates the establishment of planar cell polarity (PCP). The PCP genes *prickle* (*pk*) and *strabismus* (*stbm*) are thought to antagonize Fz signaling. We show that they act in the same cell, R4, adjacent to that in which the Fz/PCP pathway is required in the *Drosophila* eye. We demonstrate that Stbm and Pk interact physically and that Stbm recruits Pk to the cell membrane. Through this interaction, Pk affects Stbm membrane localization and can cause clustering of Stbm. Pk is also known to interact with Dsh and is thought to antagonize Dsh by affecting its membrane localization. Thus our data suggest that the Stbm/Pk complex modulates Fz/Dsh activity, resulting in a symmetry-breaking step during polarity signaling.**
*Keywords*: convergent extension/frizzled/planar cell polarity/*prickle*/*strabismus*

## Introduction

In multicellular organisms epithelia are polarized not only in the apical–basal axis, but also within the epithelial plane. In vertebrates, this epithelial planar cell polarization (PCP) is evident in the regular appearance of fish scales and bird feathers, and in internal organs such as the inner ear and the oviduct where hairs and cilia are oriented precisely with respect to each other (Eaton, 1997; Lewis and Davies, 2002; Mlodzik, 2002). In addition, the process of convergent extension (CE) during vertebrate gastrulation and neurulation shares many features and components of PCP signaling (reviewed in Myers *et al*., 2002; Wallingford *et al*., 2002a).

In *Drosophila melanogaster*, PCP is manifest in diverse structures: the hairs of wing cells all point distally, and the bristles of the thorax and the abdomen all grow in a posterior direction (Adler and Lee, 2001; Adler, 2002). In addition, the 20 cells of each ommatidium of the fly's facet eye are precisely arranged with respect to each other and to the dorsoventral and anteroposterior axes. Genetic studies have identified several genes involved in the establishment of PCP. Central to these polarity genes is the Frizzled

receptor (Fz) and the non-canonical Fz/PCP signaling pathway (Shulman *et al*., 1998; Adler, 2002; Mlodzik, 2002). It is thought that an unknown ligand leads to a Fz activity gradient. The signal is then transduced via the adapter protein Dishevelled (Theisen *et al*., 1994; Axelrod *et al*., 1998; Boutros *et al*., 1998) and small GTPases (Strutt *et al*., 1997; Fanto *et al*., 2000) to a JNK MAP kinase module, generating a transcriptional response in the eye (Paricio *et al*., 1999; Weber *et al*., 2000). In the wing and eye, the pathway leads to cytoskeletal changes involving the Rho associated kinase (Drok; Winter *et al*., 2001). Several additional genes such as *flamingo* (*fmi*; also known as *starry-night*), *diego* (*dgo*), *strabismus* (*stbm*; also known as *van-gogh*), *fat*, *dachsous* and *prickle* (*pk*) are required for PCP signaling (Heitzler *et al*., 1993; Adler *et al*., 1998; Taylor *et al*., 1998; Wolff and Rubin, 1998; Chae *et al*., 1999; Usui *et al*., 1999; Feiguin *et al*., 2001; Rawls *et al*., 2002; Yang *et al*., 2002). While the relationship of most of these genes with the Fz/PCP pathway is unclear, the atypical cadherin *fmi* can stimulate and repress Fz activity at different time points during PCP establishment (Usui *et al*., 1999; Das *et al*., 2002).

In the eye, PCP signaling specifies the R3 and R4 photoreceptor cell fates and is reflected by the mirror image arrangement of ommatidia (facets) with respect to the dorsoventral midline (equator; see also Figure 1A, B and C). This arrangement is generated by a 90° rotation of the developing ommatidial preclusters. In addition, a loss of symmetry between R3 and R4 leads to opposing chiral arrangements dorsally and ventrally of the equator (Figure 1A and B; for reviews see Wolff and Ready, 1993; Mlodzik, 1999; Reifegerste and Moses, 1999). The crucial signaling events occur as five-cell preclusters, consisting of the R8, R3/4 and R2/5 precursors, leave the morphogenetic furrow (Zheng *et al*., 1995). Higher Fz activity in the R3 relative to the R4 precursor leads to stronger activation of the JNK cascade and thus higher *Delta* (*Dl*) transcription in the R3 precursor. Dl then activates Notch (N) in the R4 precursor (Cooper and Bray, 1999; Fanto and Mlodzik, 1999; Tomlinson and Struhl, 1999). This results in increased Fmi levels and consequently repression of *Dl* expression (Das *et al*., 2002), stabilizing the R3/R4 fate decision.

PCP genes can be subdivided into two groups by their genetic requirement in the R3 or R4 precursor cells. *fz*, *dsh* and *Dl* are required in the R3 precursor cell (Zheng *et al*., 1995; Fanto and Mlodzik, 1999; Tomlinson and Struhl, 1999), while *stbm* and *N* function in R4 (Wolff and Rubin, 1998; Tomlinson and Struhl, 1999). *fmi* is the only gene required in both cells (Das *et al*., 2002). Loss-of-function (LOF) and gain-of-function (GOF) alleles of core planar polarity genes lead to ommatidia that adopt a chirality and rotate, but the acquisition of the R3/R4 fate and associated chirality occurs stochastically, and the direction and extent
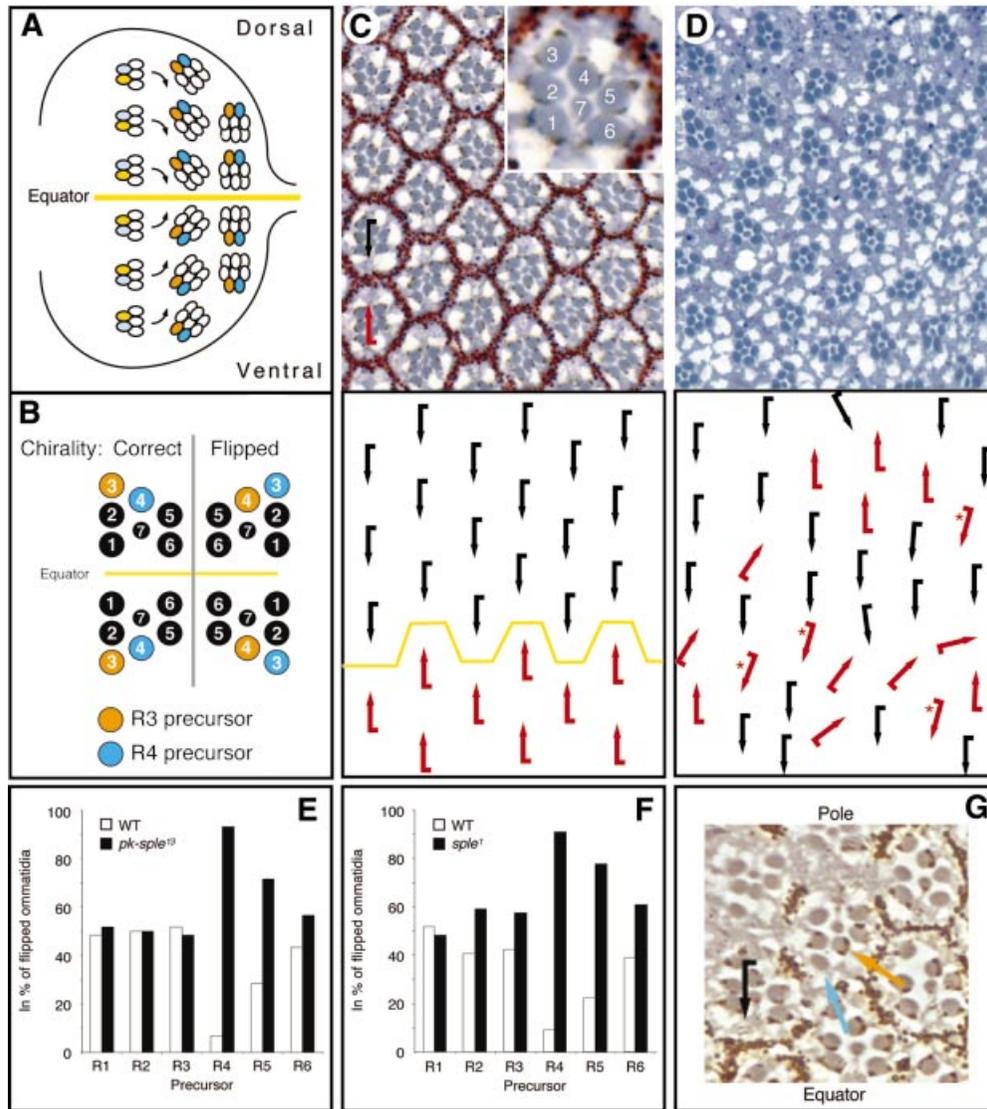
**Fig. 1.** *pk* is required in the R4 precursor cell. Anterior is left and dorsal is up. Schematic representation of ommatidial patterning in (**A**) third instar eye disk and (**B**) adult eye. Clusters rotate in opposing directions with respect to the equator (yellow line) in the eye disk (A) and acquire a dorsal or ventral chirality, as apparent in adult ommatidia (B). R3 precursors are in orange and R4 precursors in blue in both panels. In wild type, the equatorial R3 precursor becomes the anterior tip cell of the cluster, while the polar R4 precursor becomes the posterior recessed cell. Note that in the case of a chirality switch [flipped ommatidia in (B)], the R4 precursor (blue) becomes the R3 cell at the tip of the ommatidium (orange). Tangential sections of adult eyes with a schematic representation underneath are shown in (C) and (D). The insert in (C) shows an enlarged single ommatidium with numbered photoreceptors. (**C**) Wild-type eye with dorsal (black) and ventral (red arrows) chiral forms separated by equator (yellow line). (**D**) In *pk^{null}* (*pk^{pk–sple13}*), chirality is random (45 ± 3%:53 ± 1%;) and no equator is visible. Thirteen percent of all ommatidia also show rotation defects. Clonal analysis of (**E**) *pk^{null}* and (**F**) *pk^{sple1}* shows that wild-type R4 precursor cells are highly under-represented in ommatidia with wrong chirality: 267 mosaic ommatidia for *pk^{null}* (54 of which had the wrong chirality) and 416 mosaic ommatidia for *pk^{sple1}* (60 of which were flipped) were scored. Statistical analysis showed that the apparent under-representation of wild-type R5 precursors is not significant and is due to its proximity to R4 (see text). Thus *pk* activity is required only in R4. (**G**) The Pk^{Sple} isoform present in the R4 precursor only is sufficient for correct choice of chirality. All R3/R4 mosaic ommatidia with the Pk^{Sple}-expressing construct (marked autonomously by pigment granules) in R4 were wild type. In contrast, those with flipped chirality had Pk^{Sple} present in the R3 precursor (orange arrow) but not in the R4 precursor (blue arrow; because of the cell fate switch, the R4 precursor becomes R3 and takes the tip position of the ommatidium). The black arrow shows a rescued ommatidium with correct dorsal chirality.

of rotation is random. In addition, ommatidia can become symmetric.

The function of the core polarity gene *pk* in the eye and its place with respect to other PCP genes is largely unknown. *pk* encodes three protein isoforms (Pk, PkM and Sple) differing at the N-termini (Gubb *et al.*, 1999). The common part contains a PET domain, a region conserved in P̲k, E̲spinas and mouse T̲estin (Divecha and Charleston, 1995; Gubb *et al.*, 1999), followed by three LIM domains.

*pk* null mutations (*pk^{pk–sple}* class) affect PCP in all tissues. *pk^{sple}* alleles affect only the Sple isoform and show planar polarity defects in the eye and leg. The *pk^{pk}* class of alleles, which affects only the Pk isoform, shows aberrant wing hair and thorax bristle patterns (Gubb *et al.*, 1999). The PkM isoform is not expressed during PCP signaling and has no known function. At the molecular level, the PET/ LIM domain region of Pk can interact with the DEP domain and C-terminus of Dsh *in vitro* (Tree *et al.*, 2002).

It has been suggested that Pk could prevent the Fz-dependent membrane recruitment of Dsh, thereby antagonizing Fz pathway activity (Tree *et al.*, 2002).

In order to place *pk* more precisely within the PCP gene network, we used mosaic analysis and tested genetic and molecular interactions of Pk with candidate PCP genes. In contrast with previous reports (Zheng *et al.*, 1995; Gubb, 1998), we find that *pk* function is not required in R3 but is required in the R4 precursor. We show that *pk* and *stbm* interact with one another genetically and physically. Pk also affects convergent extension during gastrulation in *Xenopus*, and Pk and Stbm mutually influence their subcellular localization in animal cap cells. Our data indicate that Stbm recruits Pk to subdomains of the plasma membrane through a direct interaction. We propose that this recruitment leads to the assembly of a Stbm/Pk-containing signaling complex that alters Fz/Dsh activity and localization, thus breaking planar polarity signaling symmetry.

## Results

### *pk is required in the R4 precursor for PCP establishment in the eye*

Null alleles for *pk* ($pk^{pk–sple13}$) display a typical PCP eye phenotype: misrotations and random chirality with an associated loss of the mirror symmetry line, the equator, at the dorsoventral midline (Figure 1C and D; see also Zheng *et al.*, 1995; Gubb *et al.*, 1999). The isoform-specific alleles $pk^{sple1}$ and $pk^{pk1}$ show either a weaker phenotype or no phenotype, respectively (not shown). Thus, unlike in the wing and thorax, the complete loss of *pk* in the eye is more severe than the loss of either isoform alone (cf. Gubb, 1998; Gubb *et al.*, 1999). These defects occur early in the larva because PCP phenotypes can be detected from their earliest appreciable stage (Zheng *et al.*, 1995; Gubb *et al.*, 1999).

Although previous work has suggested that *pk* is required in the R3 precursor or in several photoreceptors (Zheng *et al.*, 1995; Gubb, 1998), we find that Pk is necessary only in the R4 precursor for normal PCP signaling to occur (Figure 1E, F and G). We performed mosaic analysis for two independent *pk* genotypes $pk^{null}$ ($pk^{pk–sple13}$; Figure 1E) and $pk^{sple1}$ (Figure 1F) and combined this with a careful statistical analysis using a logistic regression model (see below). For both genotypes, ommatidia with a wild-type R4 precursor adopted the correct chirality, whereas ommatidia with a flipped chirality rarely contained a $pk^+$ R4 precursor (Figure 1E and F; see Figure 1B for scheme; note that photoreceptor identities were assigned according to their respective precursor identity).

The only other wild-type cell that was apparently under-represented in flipped ommatidia is the R5 precursor (Figure 1E and F). We used the logistic regression model (Hosmer and Lemeshow, 1989) to assess statistically whether R5 is really required. This model takes into account that R5 has a higher probability of being of the same genotype as R4 (Tomlinson and Struhl, 1999). This analysis demonstrated that R5 is not required. Thus our data showed that only the R4 precursor genotype of *pk* correlates with the chirality decision ($p < 0.001$).

**Table I.** Quantification of genetic interactions with *sev*>Pk$^{Sple}$ and *sev*-Pk$^{Pk}$

| | *sev*>Pk$^{Sple}$ at 25°C | *sev*-Pk$^{Pk}$ at 29°C |
|---|---|---|
| w1118 (+/+ control) | 26.7 ± 5.1 | 56.4 ± 8.4 |
| $rhoA^{72o}$/+ | 26.7 ± 3.9 | 34.5 ± 3.1* |
| $stbm^{null}$/+ | 63.1 ± 8.3* | 76.2 ± 2.0* |
| $stbm^{x}$/+ | 67.4 ± 12.7* | 77.5 ± 3.8* |
| $dsh^{1}$/+ | 52.3 ± 4.4* | 63.2 ± 6.0 |
| $dsh^{v26}$/+ | 29.8 ± 0.5 | 44.4 ± 1.2 |
| $fz^{R52}$/+ | 59.3 ± 0.2* | 47.8 ± 2.7 |
| $fz^{K21}$/+ | 21.9 ± 6.5 | 34.7 ± 5.9 |
| $fmi^{E59}$/+ | 53.6 ± 10.1* | 58.9 ± 2.6 |
| $fmi^{E45}$/+ | 42.4 ± 4.5* | 52.4 ± 9.4 |
| $dgo^{308}$/+ | 56.0 ± 5.0* | 58.4 ± 5.9 |
| $dgo^{380}$/+ | 51.0 ± 14.4 | 62.0 ± 7.8 |
| $N^{55E11}$/+ | 23.2 ± 4.7 | 61.5 ± 14.4 |
| $Dl^{rev\ F10}$/+ | 41.6 ± 12.8 | 49.9 ± 1.3 |
| $drok^{1}$/+ | ND | 38.1 ± 7.3 |
| $bsk^{170b}$ FRT/+ | 21.0 ± 5.6 | ND |
| Df(3L)Pbl ($rac1^-$)/+ | 22.8 ± 11.6 | ND |
| Df(3L)Emc5 ($rac1^-$)/+ | 21.7 ± 2.4 | ND |
| FRT $jun^{2}$/+ | 27.8 ± 6.4 | ND |

Percentage of ommatidia with abnormal polarity (± standard deviation) of the analyzed eyes of flies heterozygous for the indicated alleles and containing one copy of *sev*>Pk$^{Sple}$ at 25°C (middle column) or *sev*-Pk$^{Pk}$ at 29°C (right column), respectively (*sev*-Pk$^{Pk}$ at 25°C resulted in a phenotype too weak to be scored reliably). At least 400 ommatidia of a total of three eyes were scored per genotype. The asterisks indicate significant interactions ($p \leq 0.02$, *t*-test). $dgo^{380}$ is significant only at $p \leq 0.05$ due to high variability between the different eyes. *fz* and *dsh* gave inconsistent allele-dependent results.
ND, not done.

To confirm this result we performed a mosaic analysis with a *pk* rescue construct (*sev*-Pk$^{Sple}$) in a *pk* null background. At the time of the R3/R4 fate decision, the *sevenless* (*sev*) enhancer drives gene expression in the R3/R4 precursor pair, but not the other R cells (Basler *et al.*, 1991). The *sev*-Pk$^{Sple}$ transgene fully rescues the $pk^{null}$ and $pk^{sple1}$ eye phenotype (not shown). Ommatidia mosaic for *sev*-Pk$^{Sple}$ within the R3/R4 pair (the presence of the transgene is autonomously marked by the $w^+$ pigment) were always rescued when the transgene was present in R4. In contrast, in all of the flipped R3/R4 mosaic ommatidia (48 for $pk^{null}$, 30 for $pk^{sple1}$) the rescue construct was present only in the R3 precursor that acquired the R4 fate (orange arrow in the example shown in Figure 1G). Again, the genotype of the other photoreceptors had no influence on the chirality decision. Thus we conclude that *pk* is required in R4, where *stbm* is also required, but not in the R3 precursor, which requires Fz signaling (see Introduction).

### *The Pk GOF phenotype is dominantly enhanced by stbm and vice versa*

Overexpression of either the Pk or Sple isoforms under the control of the *sev* enhancer (*sev*-Pk$^{Pk}$ and *sev*-Pk$^{Sple}$) leads to typical PCP defects: symmetric ommatidia and chirality and rotation defects (Figure 2 and Table I). These phenotypes are strongly enhanced by two alleles of *stbm*. In addition, *sev*>Pk$^{Sple}$ is also enhanced by *dgo* and two alleles of *fmi* (Figure 2A and Table I). Other genes, notably components of the MAP kinase cascade, *Dl* and *N* show no effect, suggesting that the interactions are specific.
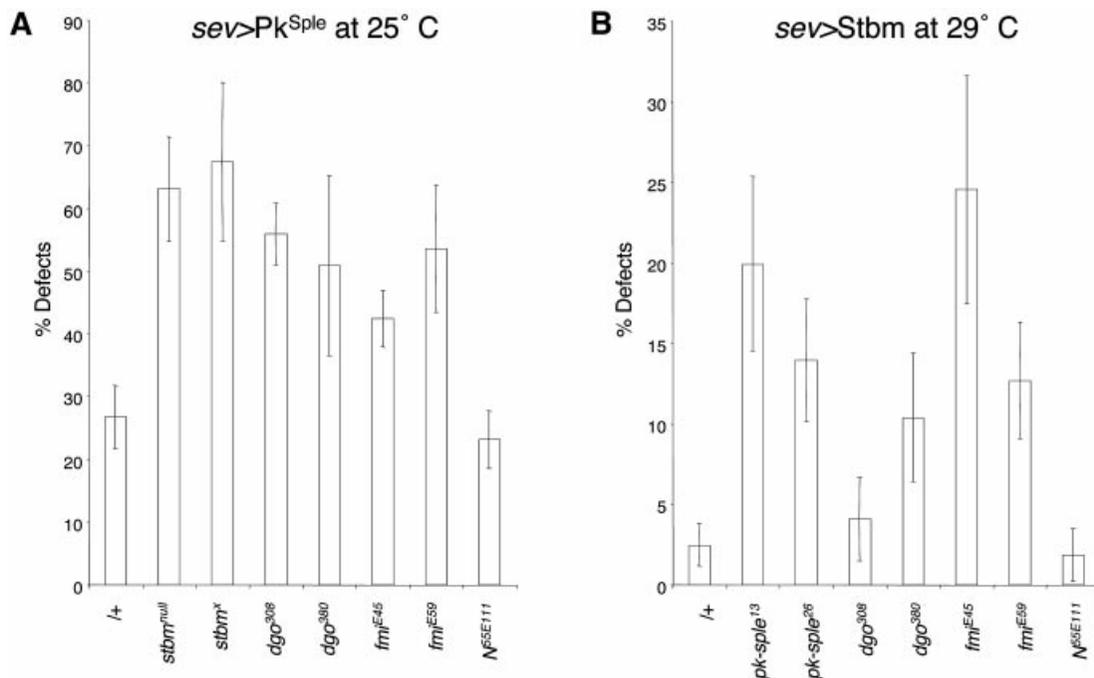
**Fig. 2.** *strabismus* and *prickle* dominantly enhance each other's GOF phenotype. The percentage of ommatidia with planar polarity defects and the standard deviation of *sev*-Gal4>*UAS*-Pk[Sple] at 25°C and *sev*-Gal4>*UAS*-Stbm at 29°C is shown in the first bar (*/+*) of panels (**A**) and (**B**), respectively. The additional bars show the effects of the removal of one copy of the respective gene indicated. The overexpression phenotype of the Sple isoform is dominantly enhanced by the removal of a copy of *stbm*, while the overexpression phenotype of Stbm is dominantly enhanced by the removal of a copy of *pk*. Both phenotypes are enhanced by removing a copy of *fmi* and *dgo*, but are unaffected by *N* (see also Table I).

Conversely, the number of affected ommatidia due to *sev*-Gal4-driven Stbm overexpression (Figure 2B) can be enhanced by the removal of one copy of *pk*, *fmi* and the stronger *dgo* allele (*dgo380*; Figure 2B). Similar dominant LOF interactions have also recently been shown between *pk*, *stbm* and *fmi* (Rawls and Wolff, 2003).

The reciprocal genetic interactions between *sev*>Stbm and *sev*>Pk[Sple], together with the requirement of both genes in R4, suggest that Pk and Stbm act together in a protein complex that requires a certain stoichiometry to function properly.

### Pk and Stbm interact with each other in vitro

Initial yeast two-hybrid data showed that Pk and Stbm interact physically with each other (A.Jenny, R.S.Darken, P.A. Wilson and M.Mlodzik, unpublished data). GST pull-down assays were used to confirm the interaction in an independent system and to map the interacting domains more precisely (Figure 3). Using *in vitro* translated deletion constructs of the region of Stbm C-terminal to the last predicted transmembrane domain (scheme in Figure 3A), we showed that a Stbm domain of less than 85 amino acids is required to interact with Pk and with Stbm itself (boxed scheme in Figure 3A).

We similarly characterized the interaction site with respect to Pk. C-terminal to the LIM domains (Pk Cterm); Pk is not highly conserved among *Drosophila*, *Xenopus* and human. However, we noted conserved stretches of basic amino acids and serine residues close to the C-terminus and a conserved C-terminal farnesylation motif [CAAX motif: KNC(I/T)IS; see alignment in

Figure 3C and scheme in Figure 3B (Zhang and Casey, 1996)]. We generated GST fusion proteins of Pk Cterm (cf. scheme in Figure 3B) and truncations thereof (e.g. lacking either the CAAX motif or the CAAX motif and the stretch of basic amino acids). We find that both the Pk–Stbm interaction and the Pk interaction with itself require a stretch of 131 amino acids close to, but not including, the very C-terminus of Pk.

To test whether the C-terminal fragments of Pk and Stbm, as well as the 131 amino acid fragment of Pk required for the interaction, show an effect *in vivo*, we expressed these fragments under the control of *sev*-Gal4. Expression of all three fragments leads to misrotated and symmetric ommatidia and chirality defects (Figure 4A, B and C). This suggests that all of these fragments can interfere with endogenous protein complex formation and, taken together with the genetic interactions between *pk* and *stbm* (see above), argues for an interference of endogenous Pk–Stbm complexes.

### Pk shows a reduced membrane association in stbm clones in the eye disk

Pk is localized in a web-like membrane-associated pattern just posterior to the morphogenetic furrow (Figure 5A′). Around ommatidial row 5, Pk shows a 'double-horse-shoe'-like pattern in R3 and R4 (Figure 5C′ and red arrow heads in Figure 5A′) and is concentrated to the equatorial side of R3 and where the R3 and R4 cell touch each other. In rows 7 and 8, Pk is often enriched in a horseshoe pattern around the R4 precursor (Figure 5D and yellow arrow-heads in Figure 5A′). Double-label studies show that Pk
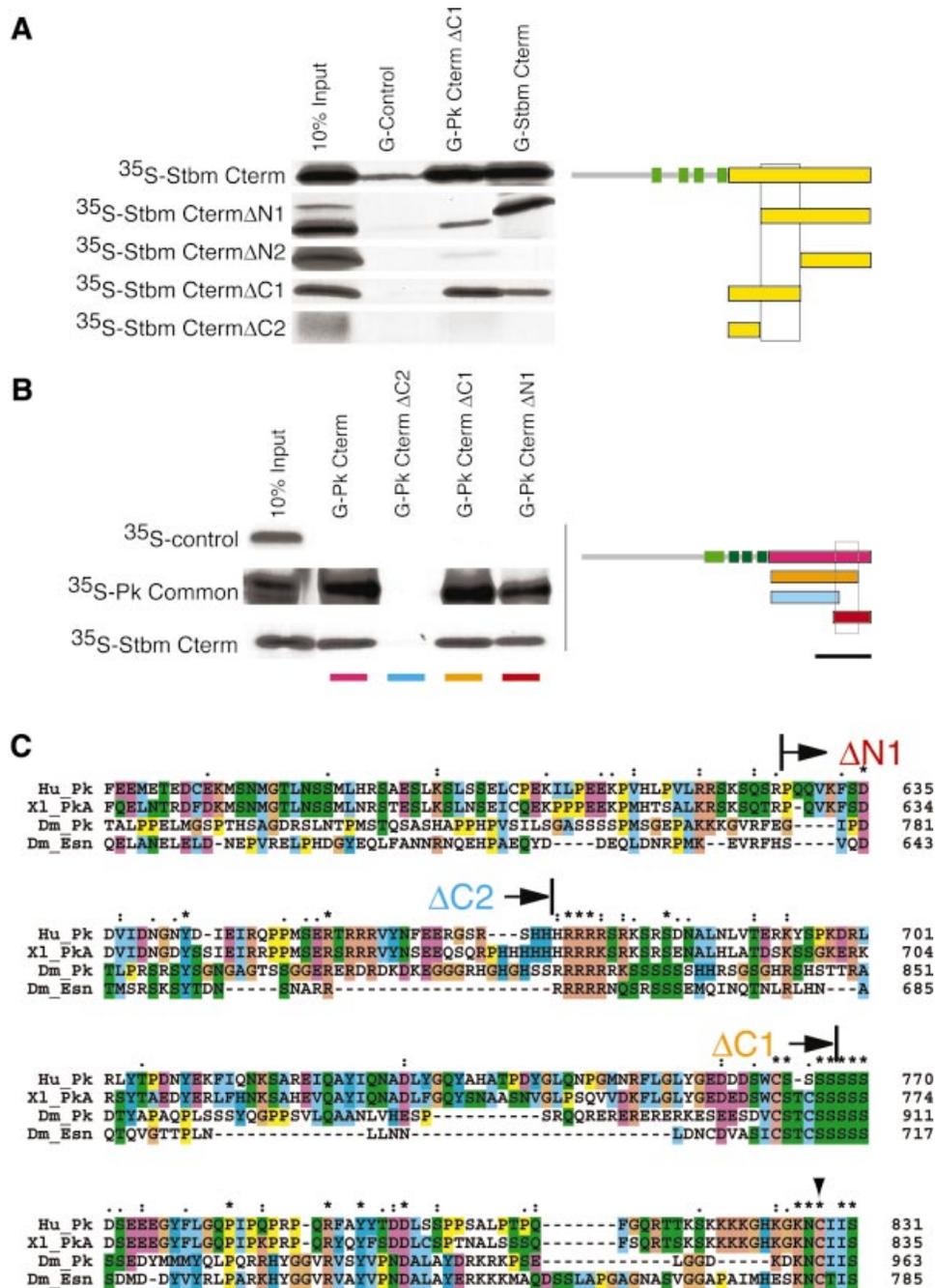
**Fig. 3.** Pk and Stbm proteins interact with each other *in vitro*. (**A**) GST fusion proteins with a fragment of the C-terminus of Pk [G-Pk CtermΔC1; orange in scheme in (B)], with the C-terminus of Stbm (G-Stbm Cterm) and with the PkM isoform specific N-terminal region (G-Control) were tested for their ability to pull down the *in vitro* translated fragments of the C-terminal region of Stbm indicated on left (marked in yellow in the scheme on the right). A fragment of 85 amino acids of the C-terminal cytoplasmic region of Stbm is required for the interaction with Pk and Stbm itself (underlaid with a box in the scheme on the right). As standard, 10% of the *in vitro* translated protein used for the pull down was loaded directly (10% input). The green boxes in the scheme indicate the four transmembrane domains. (**B**) Mapping of the binding site of Pk to Stbm and to itself. The GST fusion proteins indicated on top (color coded below, compare with scheme on right) were used to pull down the *in vitro* translated Stbm Cterm and the *in vitro* translated region common to all isoforms of Pk. A 131 amino acid fragment of Pk is required for the interaction of Pk with itself and with Stbm (underlaid with a box in scheme on right). The PkM isoform specific N-terminal region (35S-Control) is not interacting with these GST fusion proteins. As standard, 10% of the *in vitro* translated protein was loaded directly (10% input). The light and dark green boxes in the scheme indicate the positions of the PET and the three LIM domains, respectively. The bar beneath the scheme indicates the region of Pk shown in the alignment in (C). (**C**) Clustal X alignment of the C-termini of human (Hu_Pk; DDBJ/EMBL/GenBank accession No. AK056499), *X. laevis* [Xl_PkA; accession No. AF387815 (Wallingford *et al.*, 2002b)], *Drosophila* Pk (Dm_Pk; accession No. AJ243708) and the closest Pk-related *Drosophila* protein Espinas [Dm_Esn; accession No. AJ251892 (Gubb *et al.*, 1999)] spanning the interaction domain (amino acid positions given at the right). As both *Xenopus* Pk genes are almost identical, only PkA was used for the alignment. Start- or endpoints of the GST fusion proteins used in (B) are indicated above the sequences (arrows, labels color coded as in B). The region between the start of Pk-CtermΔN1 and the end of Pk-CtermΔC1 is required for the Pk inter-actions, while the CAAX motif (KNC(I/T)IS) at the very C-terminus and the serine-rich region are dispensable. The Cys mutated to Ala in the CAAX motif in *sev*-Pk^Sple–CtoA is indicated by an arrowhead.
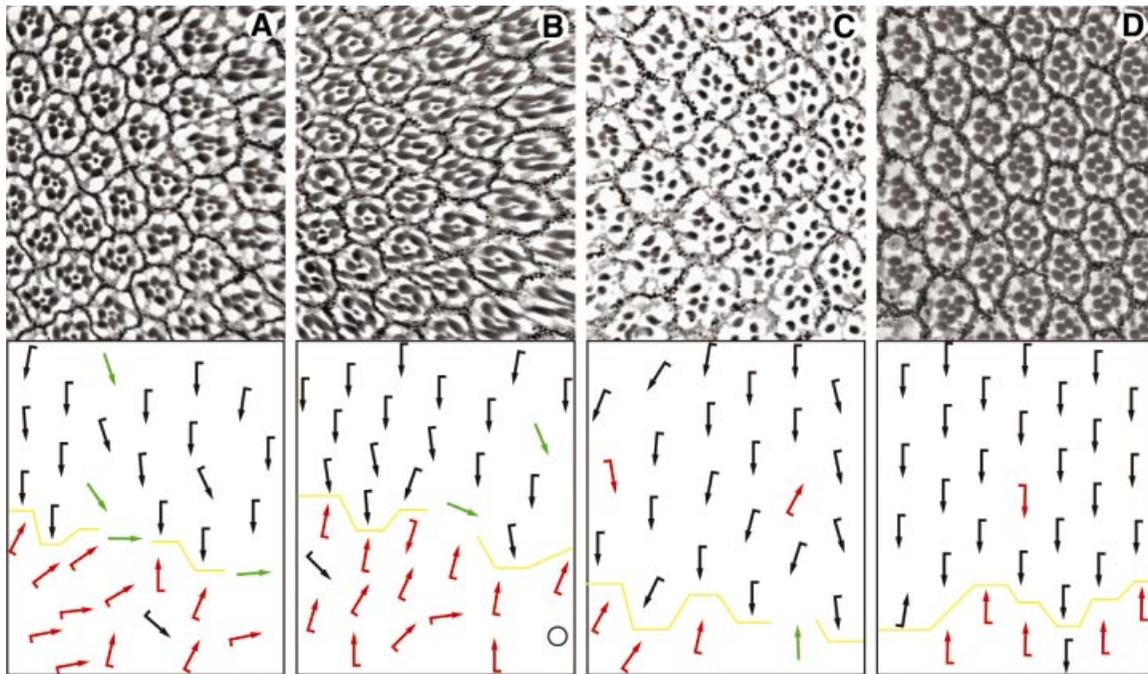
**Fig. 4.** The domains of Pk and Stbm required for interaction affect polarity *in vivo*. Tangential sections of adult eyes with a schematic representation of polarity are shown. In all panels, the equator is indicated by a yellow line and anterior is to the left. *Sev*-Gal4 was used to express the C-termini of (**A**) Pk and (**C**) Stbm and (**B**) the specific domain of Pk required for the interaction with Stbm. All three fragments perturb polarity, suggesting that the Pk–Stbm interaction is relevant for *in vivo* function. (**D**) *sev*-Pk[Sple–CtoA] which cannot be farnesylated rescues the *pk[null]* eye phenotype, suggesting that a lipid modification is not essential for Pk function in the eye.

colocalizes with Fmi (Figure 5A", C and D; Das *et al.*, 2002; Yang *et al.*, 2002) and also with Stbm (Rawls and Wolff, 2003), a prerequisite for a physiological interaction between Stbm and Pk.

Interestingly, in *stbm[null]* clones (Figure 5E) just posterior to the morphogenetic furrow, the web-like membrane staining of Pk is not seen, suggesting that Stbm is involved in the recruitment of Pk to the plasma membrane. In ommatidia of later developmental stages, Pk staining remains diffuse, but in some photoreceptor clusters one cell of the R3/R4 pair has Pk partly enriched at the cell cortex (compare yellow arrowheads with each other and with red arrowheads in Figure 5E and E′). This remaining membrane association of Pk might be explained by its CAAX farnesylation motif at the C-terminus (Figure 3C) which could contribute to membrane localization. However, as a version of Pk in which the farnesylation site had been mutated (*sev-Pk[Sple–CtoA]*) (Figure 4D) still significantly rescues a *pk[null]* mutant, farnesylation is unlikely to be essential to recruit Pk to the membrane *in vivo*. In addition, *fmi* could also contribute to Pk recruitment, as Tree and coworkers (Tree *et al.* 2002) have shown a partially reduced membrane staining of Pk in *fmi⁻* clones in wing cells.

### Pk affects convergent extension in Xenopus and can change Stbm distribution in the cell membrane

During convergent extension (CE) in vertebrates, posterior neuroectodermal and dorsal mesoderm cells acquire a bipolar cell morphology, intercalate and thus extend the body axis (for reviews see Myers *et al.*, 2002; Wallingford

*et al.*, 2002a). Mutations in zebrafish *stbm* (Jessen *et al.*, 2002) or morpholino-mediated knockout of zebrafish or *Xenopus pk* and *stbm* (Darken and Wilson, 2001; Park and Moon, 2002; Takeuchi *et al.*, 2003; Veeman *et al.*, 2003) prevent elongation of the body axis during gastrulation and neurulation without affecting cell fate. Similarly, over-expression of xFz7 and dominant negative versions of Dsh and Rok2 affect cell polarization and convergent extension in *Xenopus* (Sokol, 1996; Djiane *et al.*, 2000; Wallingford *et al.*, 2000; Marlow *et al.*, 2002). As it has been shown that overexpression of proteins affecting CE results in defects similar to their loss of function phenotypes (Darken *et al.*, 2002; Jessen *et al.*, 2002; Park and Moon, 2002), we tested whether Pk can affect CE. Compared with uninjected embryos, 87% of the embryos injected dorsally with *pk* mRNA developed with a significantly shorter dorsal axis, resulting in dorsally bent tadpoles (Figure 6A–C; quantification in Figure 6K). This effect is due to affected CE and not to altered cell fates (assessed by RT–PCR analysis; data not shown).

We also injected RNAs coding for the region common to all Pk isoforms and for Pk Cterm (cf. scheme in Figure 3), both of which strongly interfered with CE (Figure 6K). Because the interaction of Pk with Stbm maps to Pk Cterm and a related *Xenopus* construct had been shown to act in a dominant negative fashion (ΔPET/LIM; Takeuchi *et al.*, 2003), we suggest that this fragment acts like a dominant negative form and interferes with the formation of endogenous protein complexes or their localization and therefore prevents CE.

We then analyzed the subcellular distribution of Pk and Stbm in animal cap explants injected with doses lower
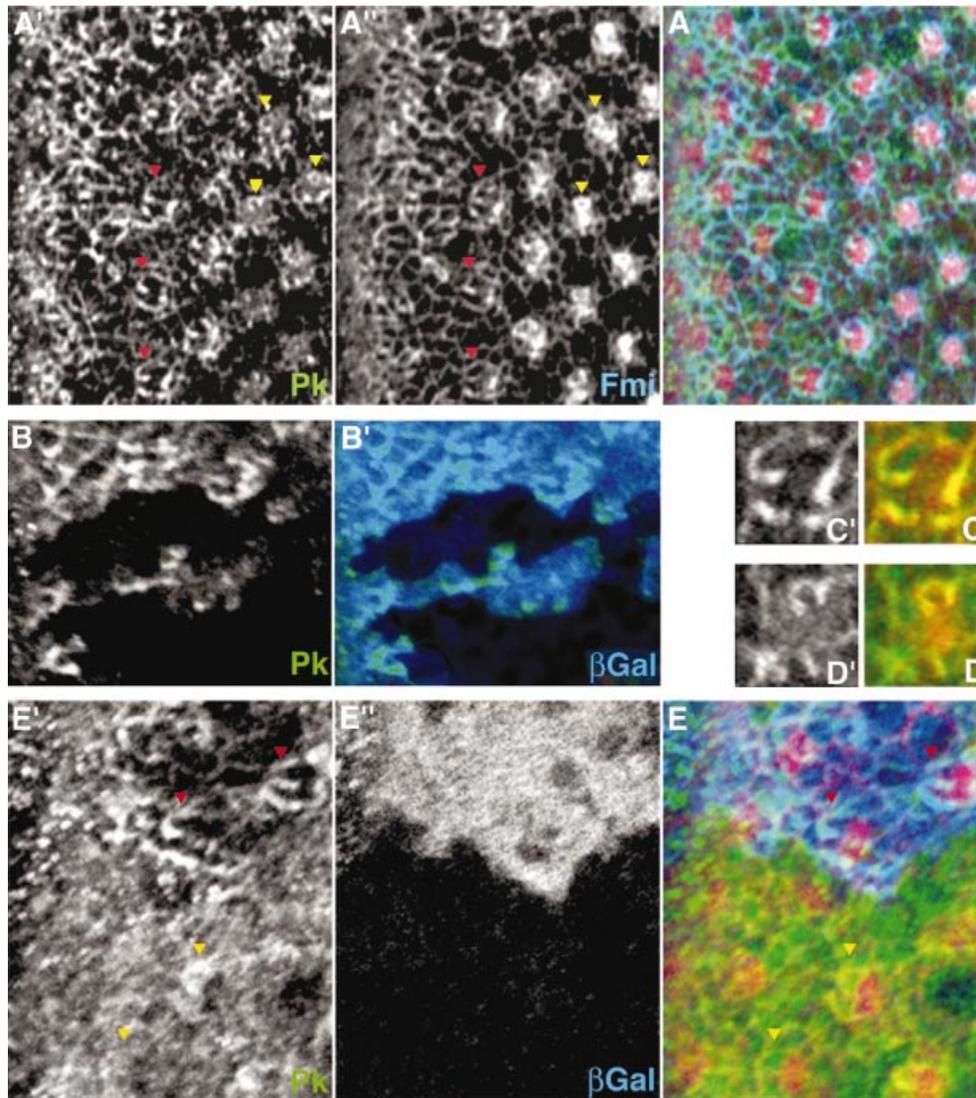
**Fig. 5.** Pk localization during polarity establishment in eye development. Confocal images of dorsal sides of third instar eye disks stained for Pk (green) are shown. (A), (C) and (D) show a wild-type disk; (B) and (E) show disks with $pk^{null}$ and $stbm^{null}$ clones, respectively. In (A) and (E), F-actin (stained with phalloidin; red) is shown as reference for the location of ommatidial preclusters. Morphogenetic furrow is at the left margin of each panel, except for (C) and (D). (**A**) Pk (A') and Fmi (A", blue in merged image) colocalize in ommatidial preclusters in R3 and/or R4 cells. Examples in row 5 (red arrowheads) and around row 7 (yellow arrowheads) are highlighted [see also (C) and (D)]. (**B**) The antibody against Pk is specific, as staining is absent from $pk^-$ clones (marked by absence of βGal staining, blue in B'). (**C** and **D**) Single photoreceptor clusters of ommatidial row 5 (C) and row 7 (D) show the 'double-horseshoe' and the horseshoe-like pattern of Pk [green and (C'), (D')], respectively. Fmi (red) colocalizes with Pk. (**E**) $stbm^{null}$ mutant clones (marked by absence of blue βGal staining in E"); Pk staining is very diffuse. In more mature clusters, partial membrane association can sometimes be detected (compare yellow arrowheads with one another and with red arrowheads).

than those required to cause phenotypic effects (see Materials and methods). GFP-Pk is primarily cytoplasmic and not concentrated at the plasma membrane (Figure 6D). GFP-xStbm is evenly distributed around the plasma membrane similar to endogenous Stbm (Figure 6F; Park and Moon, 2002). Upon coinjection of GFP-Pk with unmarked xStbm, GFP-Pk is relocalized to patches at the plasma membrane (Figure 6E). Similarly, GFP-xStbm clusters to patches in the membrane after coinjection with Pk (Figure 6G; see Supplementary data available at *The EMBO Journal* Online for a time-lapse movie). Antibody staining showed that GFP-xStbm and Pk colocalize in these patches (not shown). This indicates that Pk and Stbm can influence each other's subcellular distribution, reflecting clustering and possibly the formation of multiprotein complexes within the cell.

A GFP-Pk Cterm containing the domain that interacts with Stbm shows a distribution in the animal cap similar to Pk-GFP when injected alone (Figure 6H). Upon coinjection of xStbm, GFP-Pk Cterm is localized partially to the cell periphery. A fusion of the PET/LIM domain to GFP is unaffected by coinjection of xStbm (Figure 6J). Even though the C-terminus of Pk can be recruited to the membrane in this assay, the Pk Cterm does not induce the redistribution and clustering of Stbm/Pk into the patches seen with full-length Pk. We assume that other portions of
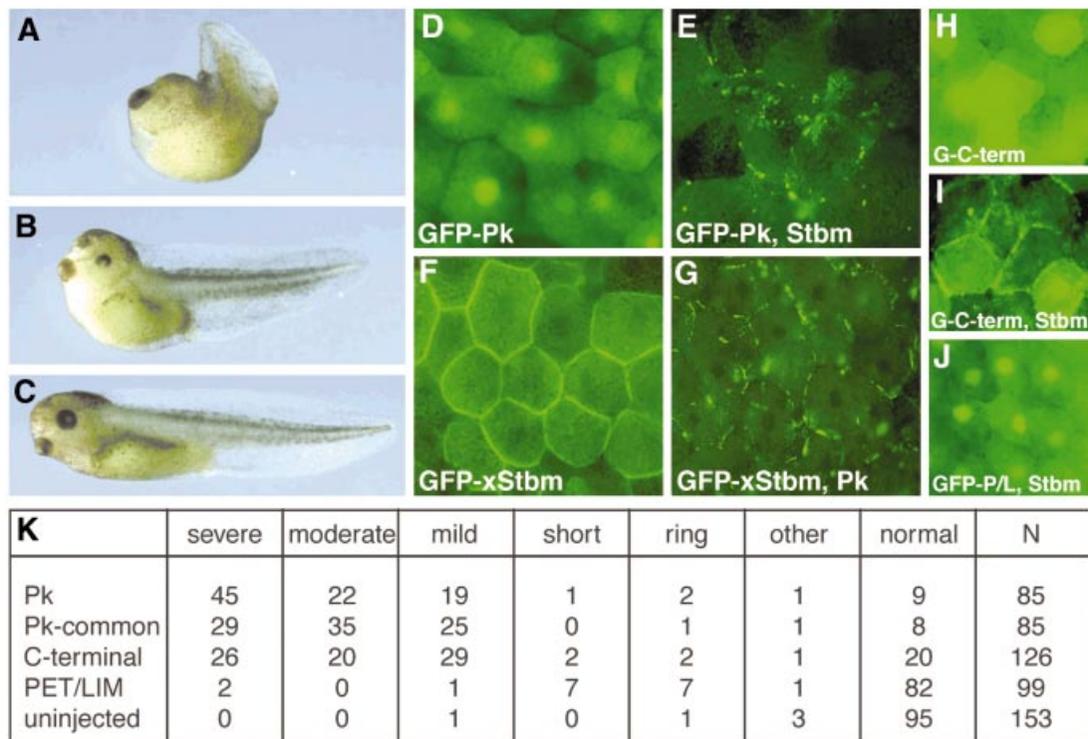
**Fig. 6.** Pk and Stbm affect each other's localization in *Xenopus*. (**A–C**) Severely (A) and moderately (B) affected tadpoles that were injected with 1 ng of *Drosophila pk* RNA bend dorsally and display a shortened dorsal axis [compared with control embryos (C)], a phenotype associated with CE defects. Embryos pictured are stage 39–40. (**D–G**) *Xenopus* Stbm and *Drosophila* Pk influence each others localization in st. 10 animal cap explants. GFP-Pk shows a mainly cytoplasmic and nuclear localization in the absence of exogenous Stbm (D), while GFP-xStbm uniformly localizes to the plasma membrane in the absence of exogenous Pk (F). Upon coinjection of unmarked xStbm, GFP-Pk is recruited into patches at the cell membrane (E). Similarly, the uniform membrane localization of GFP-xStbm becomes patchy upon coinjection of unmarked Pk (G). (**H**) GFP-Pk Cterm shows a distribution similar to GFP-Pk when injected alone. (**I**) Upon coinjection with xStbm, GFP-Pk Cterm partially localizes to the membrane. (**J**) A GFP fusion of the PET/LIM domain coinjected with xStbm is not recruited to the membrane. (**K**) Quantification of the effect of Pk fragments on CE. The percentage of embryos with CE defects after injection of 1 ng RNA, of the constructs indicated, are shown. The severe and moderate phenotypes correspond to examples shown in (A) and (B). In mildly affected embryos the head is deflected dorsally with near-normal body length, while in short embryos the overall length is decreased without obvious dorsal flexion. Embryos categorized as rings failed to close the blastopore. Embryos listed as 'other' had defects unrelated to CE. Numbers reflect the percentage of embryos in each category, except column N, corresponding to the number of injected embryos. We did not observe a defect when RNA encoding the PET/LIM region fragment was injected, but cannot exclude that the PET/LIM fragment is not translated or preferentially degraded.

Pk are required for the formation of the large patches, consistent with the idea of larger functional protein complexes.

## Discussion

In the *Drosophila* eye, PCP signaling specifies the R3 and R4 photoreceptor fates and the direction of ommatidial rotation. We show that *pk* function is required in the R4 precursor, as opposed to *fz* PCP signaling in R3, for control of polarity establishment. Stbm, a transmembrane protein also required in R4, interacts genetically and physically with Pk. This interaction is important for the recruitment of Pk to the plasma membrane. In *Xenopus* animal-cap explants, Stbm and Pk relocalize each other to subdomains of the membrane. We propose a model of how Pk/Stbm might regulate Fz/Dsh signaling activity.

### Stbm and Pk interact physically and are both required in R4

The *in vitro* molecular interaction between Pk and Stbm and their mutual relocalization in *Xenopus* animal caps suggest that they form multiprotein complexes. Several pieces of evidence indicate that the physical interaction is physiologically important: (i) correct membrane localization of Pk depends on *stbm* function because in *stbm* mutant tissue Pk staining is diffuse and absent (or strongly reduced) at the membrane (Figure 5E); (ii) Pk and Stbm interact genetically by mutually enhancing each other's GOF (this work) and LOF (Rawls and Wolff, 2003) phenotypes in the eye; (iii) *pk* is necessary for PCP signaling in the R4 precursor (this work), the same cell in which *stbm* is required (Wolff and Rubin, 1998); (iv) expression of the interacting domains (Figure 4A–C) of Pk or Stbm interferes with polarity establishment. In particular, a subfragment of 131 amino acids of the C-terminus of Pk, required for the molecular interaction, is sufficient to affect polarity.

### Potential function of the Pk/Stbm complex

Both Pk and Stbm act as if they antagonize Fz signaling. First, in zebrafish, Stbm overexpression can prevent Wnt11 from rescuing a *wnt11* mutation (Jessen *et al.*, 2002). Secondly, in the *Drosophila* wing, overexpression of Pk leads to wing hairs pointing towards the source of the overexpressed protein (Tree *et al.*, 2002), behaving like a

*fz* LOF clone (whereas overexpression of Fz leads to hairs pointing away from the Fz source). *stbm* LOF clones show the opposite behavior to *fz* LOF clones: wing hairs point away from the mutant patch, consistent with the mutant tissue having a higher Fz-activity (Taylor *et al.*, 1998).

In the *Drosophila* eye, evidence that *pk* acts antagonistically to *fz* comes from the fact that the Notch-signaling-responsive R4-specific reporter *mδ0.5-lacZ* is expressed for a prolonged period in both R3/R4 precursors in a *pkˢᵖˡᵉ¹* mutant (Cooper and Bray, 1999). This is explained if Fz activity in the R4 precursor is increased, resulting in higher levels of *Dl* there. This in turn leads to N activation and concomitant *mδ0.5-lacZ* reporter expression in both cells of the R3/R4 pair. Conversely, in *fz* and *dsh* mutant eye disks (where Fz signaling is absent or reduced and thus *Dl* should not be upregulated) N-signaling activity and *mδ-lacZ* expression is initially reduced in both cells (Cooper and Bray, 1999; Strutt *et al.*, 2002). Fz activity is also antagonized by *stbm* in the eye. Mosaic analysis of *stbm* showed that it has the capability to instruct a cell to become R4 as long as the other cell of the R3/R4 pair is mutant for *stbm* (Wolff and Rubin, 1998). Therefore, in such an all-or-nothing situation, Stbm in the R3 precursor can override a positive signal of Fz, resulting in a cell fate switch to R4 fate.

In a wild-type situation with all PCP components present in both cells, it is crucial that Stbm activity is higher in R4 than in R3 to ensure proper Fz-signaling regulation. Therefore it is an intriguing possibility that a Pk/Stbm complex in the R4 precursor ensures such higher Stbm activity, and the associated higher Fz repression there is important for a proper R3/R4 cell fate decision (see also below).

### How does the Stbm/Pk complex regulate Fz-signaling activity?

During PCP establishment in the wing, Fz, Dsh, Dgo, Fmi and Pk are initially localized uniformly around the apical circumference of wing cells (Usui *et al.*, 1999; Axelrod, 2001; Feiguin *et al.*, 2001; Shimada *et al.*, 2001; Strutt, 2001). During and after PCP signaling, these proteins relocalize and become differentially enriched: Pk concentrates on the proximal side of the cell, whereas Fz and Dsh become enriched distally. Fmi becomes enriched at both sides.

In the eye, the situation is analogous. During PCP establishment, signaling components at the R3/R4 cell border are relocalized from a uniform to a more restricted pattern. Stbm-YFP is localized on the R4 but not on the R3 side, and Fz-GFP ends up on the R3 but not the R4 side (Strutt *et al.*, 2002). The analogy between the R4/R3 and proximal/distal cell borders is corroborated by the genetic requirements in R3 and R4: the distally localized factors Dsh and Fz are required in R3, while proximally localized Pk is required in R4. Fmi is localized on both poles of each wing cell and also required in both cells of the R3 and R4 pair. The function of *fmi* has been linked to both proposed complexes, the 'Fz/Dsh side' (*fmi* is required for apical localization of both Fz and Dsh; Das *et al.*, 2002) and the Stbm/Pk complex. In addition to the genetic interactions between *fmi* and *stbm* or *pk* (Figure 2; Table I; Rawls and Wolff, 2003), a reduced membrane staining of Pk in *fmi⁻* clones in wing cells has been shown (Tree *et al.*, 2002).
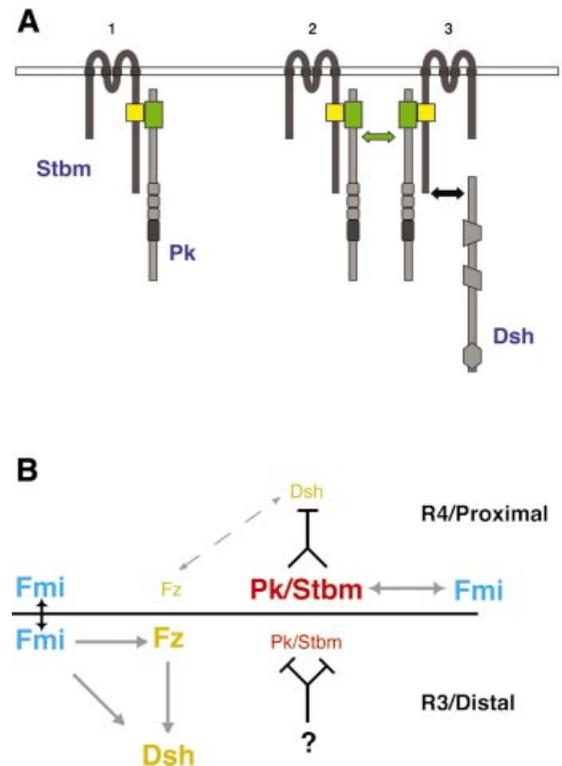


**Fig. 7.** A model for Stbm/Pk protein clustering and PCP signaling circuitry. See also text for details. (**A**) Model of how Stbm recruits Pk to the cell membrane (1) leading to its clustering (2). The complexes might then sequester Dsh from Fz signaling (3) and potentially target it for degradation. (**B**) In the R3 cell and on the distal end of a wing cell, Fz/Dsh signaling is high. Pk/Stbm is inhibited/prevented from influencing Fz/Dsh by an unknown factor. On the R4 side of the R3/R4 cell boundary and the proximal side of a wing cell, Pk/Stbm can counteract Fz/Dsh signaling (dashed arrow). Arrows: genetic (gray) and physical (black) interactions between planar polarity genes. The gene names are color coded according to their localization. See text for details.

How do these changes in localization occur? Our localization studies in *Drosophila* and *Xenopus* suggest that Pk and Stbm influence each other's localization and form clusters in subdomains of the cell membrane (Figure 7A). Interestingly, such Stbm/Pk complexes also affect Fz-dependent Dsh membrane localization (data not shown). Thus it is an intriguing possibility that the patches we observe in animal cap cells upon coinjection of Stbm with Pk represent the result of a similar, though unpolarized, symmetry-breaking step during PCP signaling.

The PET/LIM domain of Pk can interact with the DEP-domain/C-terminus of Dsh (Tree *et al.*, 2002). This interaction has been suggested to prevent Dsh membrane recruitment. Also, the C-terminus of Stbm can interact with Dsh as long as the PDZ domain is present (Park and Moon, 2002; A.Jenny, R.S.Darken, P.A.Wilson and M.Mlodzik, unpublished data). As our data suggest that Pk regulates the activity and localization of Stbm (Figure 7A), this regulation might promote or stabilize the interactions of Dsh with Stbm and/or Pk, thereby helping to pull Dsh away from a Fz-signaling complex. The Stbm/Pk complexes could then cause active release of Dsh from the membrane or target it for degradation, resulting in low levels of Dsh (and by inference Fz; Strutt, 2001) at places where Pk and Stbm are enriched (see

Figure 7B). Furthermore, in the R3 cell (or distally in the wing) an unknown factor might act to prevent either the formation of the Stbm/Pk complex or its effect on Dsh.

In conclusion, Pk and Stbm form a functional complex during PCP signaling in *Drosophila* and during convergent extension in *Xenopus*. Interestingly, in zebrafish, in addition to its function in CE, Stbm is also required for the caudal migration of hindbrain motor neurons (Jessen *et al.*, 2002). This function of Stbm is independent of Dsh and the PCP genes tested so far. It will be interesting to determine whether Stbm and Pk function together in this context as well.

## Materials and methods

### Fly strains and genetics

Mutant alleles were $w^{1118}$, $pk^{pk-sple13}$ (referred to as $pk^{null}$ in this article), $pk^{pk1}$, $pk^{sple1}$, $rho^{A72o}$, $dsh^{1}$, $dsh^{v26}$, $fz^{R52}$ $fz^{K21}$, $N^{55E11}$, $Dl^{revF10}bsk^{170b}$ FRT40, $Df(3L)Pbl$ ($rac^{1-}$), $Df(3L)Emc5$ ($rac^{1-}$), FRT42D $jun^{2}$, $\Delta2$–3Sb (all described in flybase), $fmi^{E59}$, $fmi^{E45}$ (Usui *et al.*, 1999), $dgo^{308}$, $dgo^{380}$ (Feiguin *et al.*, 2001), $stbm^{x}$ (unpublished), $stbm^{null}$ (Wolff and Rubin, 1998) and $drok^{1}$ (Winter *et al.*, 2001).

FRT42D$pk^{null}$ and FRT42D$pk^{sple1}$ were generated as described (Xu and Rubin, 1993). Eye clones were generated by the Flp/FRT technique with $ey$Flp (Newsome *et al.*, 2000) and marked with P[w$^{+}$] or arm-lacZ (Vincent *et al.*, 1994). Transgenic flies were generated by standard P-element-mediated transformation (Spradling and Rubin, 1982).

Genetic interactions were tested using the Gal4/UAS system (Brand and Perrimon, 1993) with *sev*-Gal4 (a kind gift from K.Basler) driving UAS-Sple (a kind gift from D.Gubb) and UAS-Stbm (a kind gift from T.Wolff). The effect of *sev*-Gal4>UAS-Pk$^{Pk}$ is too strong to examine genetic interactions and thus we used the weaker directly driven *sev*-Pk$^{Pk}$. Rotation was scored as defective when a cluster showed a deviation of more than 15° compared with neighboring ommatidia.

Mosaic ommatidia were analyzed to determine the genetic requirement of *pk*. Because mutant ommatidia choose chirality at random and thus can also adopt wild-type orientation, we scored genotypes of the photoreceptor precursors with wrong chirality. Note that the photoreceptor cells were numbered according to their precursor genotype, i.e. correcting for the cell fate switch (cf. Figure 1B). When the capability of *pk* to instruct a particular cell fate was assessed, the R3 and R4 reflect the position in the adult ommatidium [polar/anterior (R3) versus equatorial/posterior (R4)] and therefore not the precursor cell fate for ommatidia with wrong chirality. The genotype of the flies used for the sufficiency experiment was yw $ey$Flp;$pk^{null}$ ($cn^{+}$)/$pk^{null}$ ($cn^{+}$);*sev*-Pk$^{Sple}$/$\Delta2$–3Sb and yw $ey$Flp;$pk^{sple1}$/$pk^{sple1}$;*sev*-Pk$^{Sple}$/$\Delta2$–3Sb. Interaction crosses of *sev*>Gal4, UAS-Pk$^{Sple}$ and *sev*>Gal4, UAS-Stbm/allele of interest were grown at 29°C; *sev*-Pk$^{Pk}$/allele of interest were grown at 25°C. $w^{1118}$ was used as control.

### Histology and immunohistochemistry

Tangential sections were prepared as described (Tomlinson and Ready, 1987). Stainings of imaginal disks were performed as described (Weber *et al.*, 2000; Feiguin *et al.*, 2001), mounted in Vectashield (Vector Laboratories) and viewed on a Leica confocal microscope. Stacks of five to nine optical sections were assembled with NIH Image and Adobe Photoshop. Rat anti-ELAV (a gift from G.Rubin) was used at 1:100, anti-Pk antibody (a gift from J.Axelrod) was used at 1:500 (Tree *et al.*, 2002) and anti-Fmi (a gift from T.Uemura) was used at 1:10 (Usui *et al.*, 1999). Mouse anti-βGal (Promega) was used at 1:200, and rabbit anti-βGal (Cappel) was used at 1:2000.

### Molecular biology and biochemistry

A detailed description of the constructs used is given in the Supplementary data. The SMART program was used to predict transmembrane domains and known motifs (Schultz *et al.*, 1998). Multiple sequence alignments were made using Clustal X (Thompson *et al.*, 1997). All PCR products were either sequenced or replaced by original cDNA fragments. Silent changes were ignored.

GST fusion proteins were expressed and purified as described, except that the protein expression was induced at 30°C (Breitwieser *et al.*, 1996). Radiolabeled proteins were translated *in vitro* with the T7-coupled transcription–translation system (Promega) according to the manufacturer's instructions.

For GST pull-down experiments, 5 μg of the appropriate GST fusion protein was incubated with 15 μl pre-equilibrated glutathione–Sepharose beads (Pharmacia) in 500 μl BP [50 mM Tris–HCl pH 7.6, 150 mM KCl, 0.5% TritonX-100, 1 mM dithiotheitol and 1× EDTA free protease inhibitor cocktail (Roche)] for 30 min at 4°C on a rotating arm. The beads were then washed three times with 1 ml BP and incubated with 5 μl of an *in vitro* translation reaction in 500 μl for 1 h at 4°C. The beads were then washed three times with 1 ml BP and resuspended in 20 μl 2× concentrated SDS sample buffer. Samples were then analyzed on a 12% or 15% SDS–polyacrylamide gel. The gel was fixed, dried and exposed to a Biomax film (Kodak).

### Xenopus manipulations

Eggs were obtained and fertilized *in vitro* by standard methods and staged as described (Nieuwkoop and Faber, 1967). Cleavage stage embryos were injected in 0.5× MMR with 3.5% Ficoll using an Oxford micromanipulator and a PLI-100 Pico-Injector (Harvard Apparatus). Dorsal and ventral blastomeres were distinguished at early cleavage stages by pigmentation. Capped RNA for injection was produced *in vitro* from linearized plasmid using the Message Machine kit (Ambion). When phenotypes were analyzed, 1 ng RNA was injected. One hundred picograms of the GFP-fusion RNAs were used in the localization studies. Animal caps were cut at stage 10–10.25 using standard techniques and placed in 0.5× MMR under a coverslip with a thin layer of vacuum grease around the edge of the cover. The caps were viewed live using a Nikon Optiphot fluorescent microscope.

### Supplementary data

Supplementary data are available at *The EMBO Journal* Online.

## References

Adler,P.N. (2002) Planar signaling and morphogenesis in *Drosophila*. *Dev. Cell*, **2**, 525–535.

Adler,P.N. and Lee,H. (2001) Frizzled signaling and cell–cell interactions in planar polarity. *Curr. Opin. Cell Biol.*, **13**, 635–640.

Adler,P.N., Charlton,J. and Liu,J. (1998) Mutations in the cadherin superfamily member gene dachsous cause a tissue polarity phenotype by altering frizzled signaling. *Development*, **125**, 959–968.

Axelrod,J.D. (2001) Unipolar membrane association of Disheveled mediates Frizzled planar cell polarity signaling. *Genes Dev.*, **15**, 1182–1187.

Axelrod,J.D., Miller,J.R., Shulman,J.M., Moon,R.T. and Perrimon,N. (1998) Differential requirement of Dishevelled provides signaling specificity in the Wingless and planar cell polarity signaling pathways. *Genes Dev.*, **12**, 2610–2622.

Basler,K., Christen,B. and Hafen,E. (1991) Ligand-independent activation of the sevenless receptor tyrosine kinase changes the fate of cells in the developing *Drosophila* eye. *Cell*, **64**, 1069–1081.

Boutros,M., Paricio,N., Strutt,D.I. and Mlodzik,M. (1998) Dishevelled activates JNK and discriminates between JNK pathways in planar polarity and *wingless* signaling. *Cell*, **94**, 109–118.

Brand,A.H. and Perrimon,N. (1993) Targeted gene expression as a means of altering cell fates and generating dominant phenotypes. *Development*, **118**, 401–415.

Breitwieser,W., Markussen,F.-H., Horstmann,H. and Ephrussi,A. (1996) Oskar protein interaction with Vasa represents an essential step in polar granule assembly. *Genes Dev.*, **10**, 2179–2188.

Chae,J., Kim,M.J., Goo,J.H., Collier,S., Gubb,D., Charlton,J., Adler,P.N. and Park,W.J. (1999) The *Drosophila* tissue polarity gene starry night encodes a member of the protocadherin family. *Development*, **126**, 5421–5429.

Cooper,M.T.D. and Bray,S.J. (1999) Frizzled regulation of Notch signalling polarizes cell fate in the *Drosophila* eye. *Nature*, **397**, 526–529.

Darken,R.S. and Wilson,P.A. (2001) Axis induction by wnt signaling: target promoter responsiveness regulates competence. *Dev. Biol.*, **234**, 42–54.

Darken,R.S., Scola,A.M., Rakeman,A.S., Das,G., Mlodzik,M. and Wilson,P.A. (2002) The planar polarity gene *strabismus* regulates convergent extension movements in *Xenopus*. *EMBO J.*, **21**, 976–985.

Das,G., Reynolds-Kenneally,J. and Mlodzik,M. (2002) The atypical cadherin Flamingo links Frizzled and Notch signaling in planar polarity establishment in the *Drosophila* eye. *Dev. Cell*, **2**, 655–666.

Divecha,N. and Charleston,B. (1995) Cloning and characterisation of two new cDNAs encoding murine triple LIM domains. *Gene*, **156**, 283–286.

Djiane,A., Riou,J., Umbhauer,M., Boucaut,J. and Shi,D. (2000) Role of *frizzled 7* in the regulation of convergent extension movements during gastrulation in *Xenopus laevis*. *Development*, **127**, 3091–3100.

Eaton,S. (1997) Planar polarity in *Drosophila* and vertebrate epithelia. *Curr. Opin. Cell Biol.*, **9**, 860–866.

Fanto,M. and Mlodzik,M. (1999) Asymmetric Notch activation specifies photoreceptors R3 and R4 and planar polarity in the *Drosophila* eye. *Nature*, **397**, 523–526.

Fanto,M., Weber,U., Strutt,D.I. and Mlodzik,M. (2000) Nuclear signaling by Rac abd Rho GTPases is required in the establishment of epithelial planar polarity in the *Drosophila* eye. *Curr. Biol.*, **10**, 979–988.

Feiguin,F., Hannus,M., Mlodzik,M. and Eaton,S. (2001) The Ankyrin repeat protein Diego mediates Frizzled-dependent planar polarization. *Dev. Cell*, **1**, 93–101.

Gubb,D. (1998) Cellular polarity, mitotic synchrony and axes of symmetry during growth. Where does the information come from? *Int. J. Dev. Biol.*, **42**, 369–377.

Gubb,D., Green,C., Huen,D., Coulson,D., Johnson,G., Tree,D., Collier,S. and Roote,J. (1999) The balance between isoforms of the *prickle* LIM domain protein is critical for planar polarity in *Drosophila* imaginal discs. *Genes Dev.*, **13**, 2315–2327.

Heitzler,P., Coulson,D., Saenz-Robles,M.T., Ashburner,M., Roote,J., Simpson,P. and Gubb,D. (1993) Genetic and cytogenetic analysis of the 43A-E region containing the segment polarity gene *costa* and the cellular polarity genes *prickle* and *spiny-legs* in *Drosophila melanogaster*. *Genetics*, **135**, 105–115.

Hosmer,D.W. and Lemeshow,S. (1989) *Applied Logistic Regression*. Wiley, New York, NY.

Jessen,J.R., Topczewski,J., Bingham,S., Sepich,D.S., Marlow,F., Chandrasekhar,A. and Solnica-Kerzel,L. (2002) Zebrafish *trilobite* indentifies new roles for Strabismus in gastrulation and neuronal movements. *Nat. Cell. Biol.*, **4**, 610–615.

Lewis,J. and Davies,A. (2002) Planar cell polarity in the inner ear: how do hair cells acquire their oriented structure? *J. Neurobiol.*, **53**, 190–201.

Marlow,F., Topczewski,J., Sepich,D. and Solnica-Krezel,L. (2002) Zebrafish rho kinase 2 acts downstream of wnt11 to mediate cell polarity and effective convergence and extension movements. *Curr. Biol.*, **12**, 876–884.

Mlodzik,M. (1999) Planar polarity in the *Drosophila* eye: a multifaceted view of signaling specificity and cross-talk. *EMBO J.*, **18**, 6873–6879.

Mlodzik,M. (2002) Planar cell polarization: do the same mechanisms regulate *Drosophila* tissue polarity and vertebrate gastrulation? *Trends Genet.*, **18**, 564–571.

Myers,D., Sepich,D.S. and Solnica-Kerzel,L. (2002) Convergence and extension in vertebrate gastrulae: cell movements according to or in search of identity? *Trends Genet.*, **18**, 447–455.

Newsome,T.P., Asling,B. and Dickson,B.J. (2000) Analysis of *Drosophila* photoreceptor axon guidance in eye-specific mosaics. *Development*, **127**, 851–860.

Nieuwkoop,P.D. and Faber,J. (1967) *Normal Table of Xenopus Laevis (Daudin)*. North-Holland, Amsterdam, The Netherlands.

Paricio,N., Feiguin,F., Boutros,M., Eaton,S. and Mlodzik,M. (1999) The *Drosophila* STE20-like kinase Misshapen is required downstream of the Frizzled receptor in planar polarity signaling. *EMBO J.*, **18**, 4669–4678.

Park,M. and Moon,R.T. (2002) The planar cell polarity gene *stbm*

regulates cell behaviour and cell fate in vertebrate embryos. *Nat. Cell Biol.*, **4**, 20–25.

Rawls,A.S. and Wolff,T. (2003) Strabismus requires Flamingo and Prickle function to regulate tissue polarity in the *Drosophila* eye. *Development*, **130**, 1877–1887.

Rawls,A.S., Guinto,J.B. and Wolff,T. (2002) The cadherins fat and dachsous regulate dorsal/ventral signaling in the *Drosophila* eye. *Curr. Biol.*, **12**, 1021–1026.

Reifegerste,R. and Moses,K. (1999) The genetics of epithelial polarity and pattern in the *Drosophila* retina. *BioEssays*, **21**, 275–285.

Schultz,J., Milpetz,F., Bork,P. and Ponting,C.P. (1998) SMART, a simple modular architecture research tool: identification of signaling domains. *Proc. Natl Acad. Sci. USA*, **95**, 5857–5864.

Shimada,Y., Usui,T., Yanagawa,S., Takeichi,M. and Uemura,T. (2001) Asymmetric colocalization of Flamingo, a seven-pass transmembrane cadherin and Dishevelled in planar cell polarization. *Curr. Biol.*, **11**, 859–863.

Shulman,J.M., Perrimon,N. and Axelrod,J.D. (1998) Frizzled signaling and the developmental control of cell polarity. *Trends Genet.*, **14**, 452–458.

Sokol,S.Y. (1996) Analysis of Dishevelled signalling pathways during *Xenopus* development. *Curr. Biol.*, **6**, 1456–1467.

Spradling,A.C. and Rubin,G.M. (1982) Transposition of cloned P-elements into *Drosophila* germ line chromosomes. *Science*, **218**, 341–347.

Strutt,D.I. (2001) Asymmetric localization of frizzled and the establishment of cell polarity in the *Drosophila* wing. *Mol. Cell*, **7**, 367–375.

Strutt,D.I., Weber,U. and Mlodzik,M. (1997) The role of RhoA in tissue polarity and Frizzled signalling. *Nature*, **387**, 292–295.

Strutt,D., Johnson,R., Cooper,K. and Bray,S. (2002) Asymmetric localization of frizzled and the determination of notch-dependent cell fate in the *Drosophila* eye. *Curr. Biol.*, **12**, 813–824.

Takeuchi,M., Nakabayashi,J., Sakaguchi,T., Yamamoto,T.S., Takahashi,H., Takeda,H. and Ueno,N. (2003) The prickle-related gene in vertebrates is essential for gastrulation cell movements. *Curr. Biol.*, **13**, 674–679.

Taylor,J., Abramova,N., Charlton,J. and Adler,P.N. (1998) Van Gogh: a new *Drosophila* tissue polarity gene. *Genetics*, **150**, 199–210.

Theisen,H., Purcell,J., Bennett,M., Kansagara,D., Syed,A. and Marsh,J.L. (1994) *dishevelled* is required during *wingless* signalling to establish both cell polarity and cell identity. *Development*, **120**, 347–360.

Thompson,J.D., Gibson,T.J., Plewniak,F., Jeanmougin,F. and Higgins,D.G. (1997) The Clustal X windows interface: flexible strategies for multiple sequence alignment aided by quality analysis tools. *Nucleic Acids Res.*, **25**, 4876–4882.

Tomlinson,A. and Ready,D.F. (1987) Cell fate in the *Drosophila* ommatidium. *Dev. Biol.*, **123**, 264–275.

Tomlinson,A. and Struhl,G. (1999) Decoding vectorial information from a gradient: sequential roles of the receptors Frizzled and Notch in establishing planar polarity in the *Drosophila* eye. *Development*, **126**, 5725–5738.

Tree,D.R.P., Shulman,J.M., Rousset,R., Scott,M.P., Gubb,D. and Axelrod,J.D. (2002) Prickle mediates feedback amplification to generate asymmetric planar cell polarity signaling. *Cell*, **109**, 371–381.

Usui,T., Shima,Y., Shimada,Y., Hirano,S., Burgess,R.W., Schwarz,T.L., Takeichi,M. and Uemura,T. (1999) Flamingo, a seven-pass transmembrane cadherin, regulates planar cell polarity under the control of Frizzled. *Cell*, **98**, 585–595.

Veeman,M.T., Slusarski,D.C., Kaykas,A., Louie,S.H. and Moon,R.T. (2003) Zebrafish *prickle*, a modulator of noncanonical *wnt/fz* signaling, regulates gastrulation movements. *Curr. Biol.*, **13**, 680–685.

Vincent,J.-P., Girdham,C.H. and O'Farrell,P.H. (1994) A cell-autonomous, ubiquitous marker for the analysis of *Drosophila* genetic mosaics. *Dev. Biol.*, **164**, 328–331.

Wallingford,J.B., Rowning,B.A., Vogeli,K.M., Rothbacher,U., Fraser,S.E. and Harland,R.M. (2000) Dishevelled controls cell polarity during *Xenopus* gastrulation. *Nature*, **405**, 81–85.

Wallingford,J.B., Fraser,S.E. and Harland,R.M. (2002a) Convergent extension: the molecular control of polarized cell movement during embryonic development. *Dev. Cell*, **2**, 695–706.

Wallingford,J.B., Goto,T., Keller,R. and Harland,R.M. (2002b) Cloning and expression of *Xenopus* Prickle, an orthologue of a *Drosophila* planar cell polarity gene. *Mech. Dev.*, **116**, 183–186.

Weber,U., Paricio,N. and Mlodzik,M. (2000) Jun mediates Frizzled

induced R3/R4 cell fate distinction and planar polarity determination in the *Drosophila* eye. *Development*, **127**, 3619–3629.

Winter,C.G., Wang,B., Ballew,A., Royou,A., Karess,R., Axelrod,J.D. and Luo,L. (2001) *Drosophila* Rho-associated kinase (Drok) links Frizzled-mediated planar cell polarity signaling to the actin cytoskeleton. *Cell*, **105**, 81–91.

Wolff,T. and Ready,D.F. (1993) Pattern formation in the *Drosophila* retina. In Martinez-Arias,M.B.A. (ed.), *The Development of Drosophila melanogaster*. Cold Spring Harbor Press, Cold Spring Harbor, NY, pp. 1277–1326.

Wolff,T. and Rubin,G.M. (1998) *strabismus*, a novel gene that regulates tissue polarity and cell fate decisions in *Drosophila*. *Development*, **125**, 1149–1159.

Xu,T. and Rubin,G.M. (1993) Analysis of genetic mosaics in developing and adult *Drosophila* tissues. *Development*, **117**, 1223–1237.

Yang,C., Axelrod,J.D. and Simon,M.A. (2002) Regulation of Frizzled by Fat-like cadherins during planar polarity signaling in the *Drosophila* compound eye. *Cell*, **108**, 675–688.

Zhang,F.L. and Casey,P. (1996) Protein prenylation: molecular mechanisms and functional consequences. *Annu. Rev. Biochem.*, **65**, 241–269.

Zheng,L., Zhang,J. and Carthew,R.W. (1995) *frizzled* regulates mirror-symmetric pattern formation in the *Drosophila* eye. *Development*, **121**, 3045–3055.

## Note added in proof

Bastock *et al.* have also recently reported an association of Stbm and Pk [Bastock,H., Strutt,H. and Strutt,D. (2003) Strabismus is asymmetrically localised and binds to Prickle and Dishevelled during *Drosophila* planar polarity patterning. *Development*, **130**, 3007–3014].